npg

www.nature.com/cddis

The role of reactive oxygen species and autophagy in safingol-induced cell death

L-U Ling[1], K-B Tan[1], H Lin[1] and GNC Chiu*,[1]

Safingol is a sphingolipid with promising anticancer potential, which is currently in phase I clinical trial. Yet, the underlying mechanisms of its action remain largely unknown. We reported here that safingol-induced primarily accidental necrotic cell death in MDA-MB-231 and HT-29 cells, as shown by the increase in the percentage of cells stained positive for 7-aminoactinomycin D, collapse of mitochondria membrane potential and depletion of intracellular ATP. Importantly, safingol treatment produced time- and concentration-dependent reactive oxygen species (ROS) generation. Autophagy was triggered following safingol treatment, as reflected by the formation of autophagosomes, acidic vacuoles, increased light chain 3-II and Atg biomarkers expression. Interestingly, scavenging ROS with N-acetyl-L-cysteine could prevent the autophagic features and reverse safingol-induced necrosis. Our data also suggested that autophagy was a cell repair mechanism, as suppression of autophagy by 3-methyladenine or bafilomycin A1 significantly augmented cell death on 2-5 μM safingol treatment. In addition, Bcl-xL and Bax might be involved in the regulation of safingol-induced autophagy. Finally, glucose uptake was shown to be inhibited by safingol treatment, which was associated with an increase in p-AMPK expression. Taken together, our data suggested that ROS was the mediator of safingol-induced cancer cell death, and autophagy is likely to be a mechanism triggered to repair damages from ROS generation on safingol treatment.
Cell Death and Disease (2011) **2,** e129; doi:10.1038/cddis.2011.12; published online 10 March 2011

Oxidative stress occurs in cells when an imbalance exists to favor the production of reactive oxygen species (ROS), such as superoxide (O_2^-), hydroxyl radical ($HO^\bullet$) and hydrogen peroxide (H_2O_2) over antioxidant defenses.[1] Oxidative stress has been implicated in a number of human physiological and pathological processes, including cancer, ischemic injury, neurodegenerative diseases, chronic inflammation, type II diabetes and arteriosclerosis. ROS is recognized as a central mediator in deciding the fate of a cell, depending on the extent of oxidative damage.[2] Under physiological conditions, low levels of ROS activate various cellular signaling molecules, such as tyrosine kinase, mitogen-activated protein kinase, small Ras proteins, nuclear factor kappa B (NF-κB) and hypoxia-inducible factor α, leading to growth adaptation and survival.[2] In contrast, excessive production of ROS causes irreversible damage to lipids, DNA and proteins, thus provoking cell death through several modes, including apoptosis and necrosis.[2] Cancer cells with their higher metabolic rate even at basal conditions would result in high intracellular ROS concentrations. This in turn makes cancer cells under increased oxidative stress and more vulnerable to ROS-mediated insults and cell death.

Apoptosis is the best-described type of programmed cell death, which is characterized by distinct morphologic features, such as cell membrane blebbing, reduction of cellular volume, activation of caspases, chromatin condensation and nuclear fragmentation.[3] Necrosis, on the other hand, is less well-characterized and associated with features including rupture of cell plasma membrane, loss of mitochondria membrane potential (MMP), depletion of adenosine triphosphate (ATP) levels and overproduction of ROS.[3] For a long time, necrosis is considered as an accidental form of cell death. However, accumulating evidence over the last decade supports a sequence of events that characterize necrosis, which could involve death receptors and receptor-interacting protein 1 (RIP1) kinase.[4] Recently, ROS is also shown to regulate autophagy,[5] a catabolic process, which is not only involved in energy homeostasis, organelle turnover and development, but also in cancer cell death.[3] Various ROS-generating drugs have proven to be effective in cancer research by causing mitochondria damage and cell death.

Safingol ((2S, 3S)-2-amino-1,3-octadecanediol) is a saturated analog of sphingosine that belongs to the family of sphingolipids.[6–8] Safingol is currently under a phase I clinical trial in combination with cisplatin for the treatment of advanced solid tumors.[9] In addition, several *in vitro* and *in vivo* studies demonstrated that safingol augmented the efficacy of other chemotherapeutic agents, including fenretinide, 1-β-D-arabinofuranosylcytosine, cisplatin, vinblastine, irinotecan and mitomycin-C in a variety of tumor cell lines.[7,10–15] Despite

[1]Department of Pharmacy, Faculty of Science, National University of Singapore, Singapore, Singapore
*Corresponding author: GNC Chiu, Department of Pharmacy, Faculty of Science, National University of Singapore, Block S4, 02-09, 18 Science Drive 4, Singapore 117543, Singapore. Tel: + 656 516 5536; Fax: + 656 779 1554; E-mail: phacncg@nus.edu.sg

of the accumulating evidence suggesting the therapeutic potential of safingol, the underlying mechanism of safingol remains largely unknown.

The cytotoxic effect of safingol was previously shown to be attributed to the inhibition of sphingosine kinase, thus preventing the formation of sphingosine-1-phosphate, which is involved in cell proliferation, invasion and angiogenesis.[6] In addition, safingol was also reported to inhibit protein kinase C (PKC) by displacing phorbol dibutyrate from PKC regulatory domain.[8,16] However, we[15] and others[10,17] have shown that PKC inhibition may not be the primary mechanism by which safingol induces cell death, particularly at clinically achievable concentrations ($\leqslant 10 \mu M$). Recent investigations shed new light that safingol could induce cell death associated with autophagic features.[17,18] Furthermore, modulations of Bcl-2 family proteins, such as Bim and Bcl-xL[19] as well as endonuclease G from mitochondria were also implicated in safingol-induced cell death at 10–50 μM safingol.[19,20] At present, there are two main questions remain unanswered. First, the role of ROS in safingol-treated cancer cells is yet to be explored. Several reports have demonstrated that safingol induced ROS production in fungi and plant cells,[21,22] yet no studies have been performed in human cancer cells. Moreover, bioactive lipids, such as ceramide were reported to induce ROS production in lymphoid cells.[23] Second, the role and regulation of autophagy in safingol-treated cells remain elusive, as modulation or inhibition of safingol-induced autophagy has not been correlated with an increase or decrease in cell death. A recent breakthrough revealed that Bcl-2 family proteins including Bcl-2, Bcl-xL and Bax regulate autophagy,[24,25] despite the well-established role of these proteins in apoptosis. Increasing evidence shows a link between ROS and autophagy, in which ROS generation could trigger autophagy.[5] Therefore, in this study, we sought to elucidate the role of ROS and autophagy in determining the fate of safingol-treated cells. Here, we identify that ROS has a critical role in causing cell death by necrosis in safingol-treated cells, and autophagy is induced as a cell repair mechanism to counteract the damaging effect caused by ROS.

Results

Safingol induced necrosis in MDA-MB-231 and HT-29 cells. Previously, safingol was shown to induce cell death in a caspase-independent manner,[17,19,20,26] and we could obtain similar results in MDA-MB-231 and HT-29 cells with specific inhibitors to caspases 8 and 9 and pan-caspase inhibitor (data not shown). In order to characterize the mechanism by which safingol exerts its cell killing effect, we performed flow cytometric analysis after staining the cells with annexin V-FITC/7-aminoactinomycin D (7AAD). Paraformaldehyde 2% was included as a positive control for inducing necrosis in cells. No significant increase in the percentage of cells stained positive for annexin V-FITC was observed in MDA-MB-231 and HT-29 cells after a 48-h exposure to safingol (Figure 1a). In contrast, concentration-dependent increase in the percentage of cells stained positive for 7AAD was observed (Figure 1a), indicating a

loss of cell membrane integrity that is suggestive of necrotic cell death. A shorter treatment time of 24 h with 10 μM safingol yielded similar results (Figure 1 inset), indicating that plasma membrane permeabilization, as reflected by 7AAD positivity, occurred early on as opposed to delayed occurrence that is associated with late-stage apoptosis. As the loss of MMP and depletion of ATP have been described as the hallmarks of necrosis,[3,4] we further performed measurements on these two biochemical events. Remarkable loss of MMP in HT-29 cells was observed after a 48-h exposure to 10 μM safingol (Figure 1b). Significant depletion of cellular ATP was also observed in both cell lines with 10 μM safingol (Figure 1c). Taken together, these data suggest that necrosis, rather than apoptosis, is the main mode through which cancer cell death occurred on safingol treatment. We further examined whether the execution of necrotic cell death is a programmed event that involves RIP1 kinase. Cells were exposed to safingol with or without necrostatin-1, a small molecule inhibitor of RIP1 kinase.[27] Our results indicated that necrostatin-1 did not prevent safingol-induced cell death (Figure 1d), thus suggesting an accidental form of necrotic cell death.

Exposure to safingol triggered ROS generation. In light of previous findings that safingol could induce ROS generation in fungi and plant cells,[21,22] we were interested to probe if ROS would be generated in cancer cells on safingol treatment. MDA-MB-231 and HT-29 cells were loaded with the ROS probe, 2′,7′-dichlorodihydrofluorescein diacetate (H$_2$DCFDA), and H$_2$O$_2$ was included as a positive control. As shown in Figure 2, safingol-induced ROS generation in a time- and concentration-dependent manner, as reflected by the increase in fluorescence intensity. The highest amount of ROS was generated after 8 h of exposure to 10 μM safingol, with $\sim$11- and 7-fold increases over untreated control in MDA-MB-231 and HT-29 cells, respectively (Figures 2a and b).

ROS triggered induction of autophagy in MDA-MB-231 and HT-29 cells. On the basis of the results presented in Figure 2, we postulated that autophagy would be triggered in the cancer cells on safingol treatment, as ROS could induce cellular damages.[2] As demonstrated through the ultrastructural morphology using transmission electron microscopy, safingol-treated MDA-MB-231 and HT-29 cells displayed characteristic autophagosomes, as well as cytoplasmic vacuoles (Figure 3a). Concentration-dependent formation of acidic vesicular organelles (AVOs) could be observed in safingol-treated cells when stained with the lysosomo-tropic agent, acridine orange,[28] and formation of AVO was markedly suppressed in both cell lines in the presence of 1 mM 3-methyladenine (3-MA), the most commonly used autophagy inhibitor[29] (Figure 3b). Induction of autophagy is further supported by the conversion of light chain 3 (LC3)-I to LC3-II in a concentration- and time-dependent manner on safingol treatment in the two cell lines (Figures 3c and d). A trend of increasing expression of the Atg proteins (Atg 5, 7 and 12) in MDA-MB-231 and HT-29 cells over the course of 48 h was also observed on safingol treatment (Figure 3d). Importantly, in the presence of the
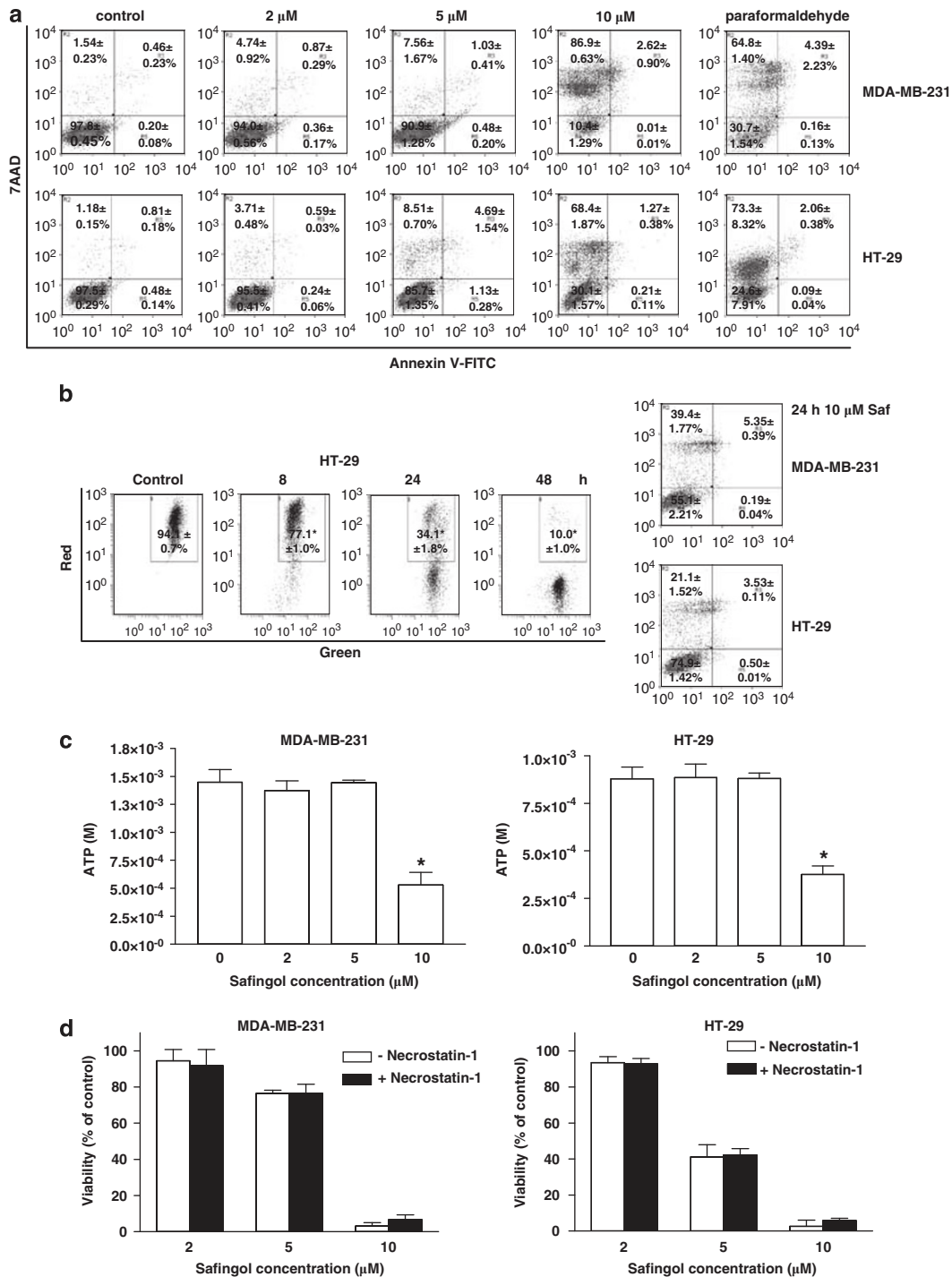
Figure 1 Cell death mechanism induced by safingol treatment in MDA-MB-231 and HT-29 cells. (**a**) Flow cytometric analysis of MDA-MB-231 and HT-29 cells after 2, 5 and 10 μM safingol treatment for 48 h. In all, 2% paraformaldehyde was used as a positive control to induce necrosis. Cells were harvested and stained with annexin V-FITC/7AAD before analyzed by flow cytometry. Results from treatment with 10 μM safingol for 24 h in the two cell lines are shown in the inset. Each reported value represents the mean ± S.E.M. from three independent experiments. (**b**) Effect of safingol on MMP in HT-29 cells. Cells were treated with 10 μM safingol for 8, 24 and 48 h, stained with JC-1 and subjected to flow cytometry. Representative dot plots from three independent experiments were shown, and numerical values represent means ± S.E.M. ($n = 3$). (**c**) Effect of safingol on intracellular ATP. Cells were treated with 2, 5 and 10 μM safingol for 48 h before measurement of ATP by a luminometric assay. Results shown are means ± S.E.M. from three independent experiments. (**d**) Effect of necrostatin-1 on the viability of safingol-treated cells. Cells were treated with safingol ± 100 μM necrostatin-1 for 48 h. Viability was assessed using MTT assay. Results shown are means ± S.E.M. from three independent experiments. *$P < 0.05$, compared with untreated control

ROS scavenger, *N*-acetyl-L-cysteine (NAC), marked reduction in the formation of AVO and in the conversion of LC3-I to LC3-II could be demonstrated in MDA-MB-231 and HT-29 cells (Figures 4a and b). Taken together, our results have demonstrated that safingol is capable of inducing autophagy, which are in line with two recent reports,[17,18] and that autophagy is induced as a result of ROS generation on safingol treatment.

The role of autophagy and ROS in safingol-treated MDA-MB-231 and HT-29 cells. Increased autophagic activity has been suggested to associate with cell death despite a lack of causative relationship of these two events.[3] On the other hand, cell death could be accelerated when autophagy is suppressed, suggesting a pro-survival role of autophagy.[3] To assess the role of autophagy in safingol-induced cancer cell

death, we have used two different pharmacological inhibitors of autophagy, 3-MA and bafilomycin A1 (BA1), which act at different points of the autophagic pathway.[29,30] Viability was > 85% of control when the cancer cells were exposed to 3-MA or BA1 alone. Suppression of autophagy by the inhibitors did not block cell death brought about by 2 or 5 μM safingol (Figure 5a). On the contrary, significant augmentation in cell death was observed on autophagy suppression. At the highest concentration of safingol tested (10 μM), the presence of 3-MA or BA1 did not impart any significant effect on cell viability (Figure 5a). These findings suggest that low concentrations (2–5 μM) of safingol induced low levels of ROS and damage whereby the autophagic pathway could possibly degrade the damaged cellular components. In contrast, it is possible that a high concentration of safingol-induced significant levels of ROS and damage that is beyond repair. Further studies
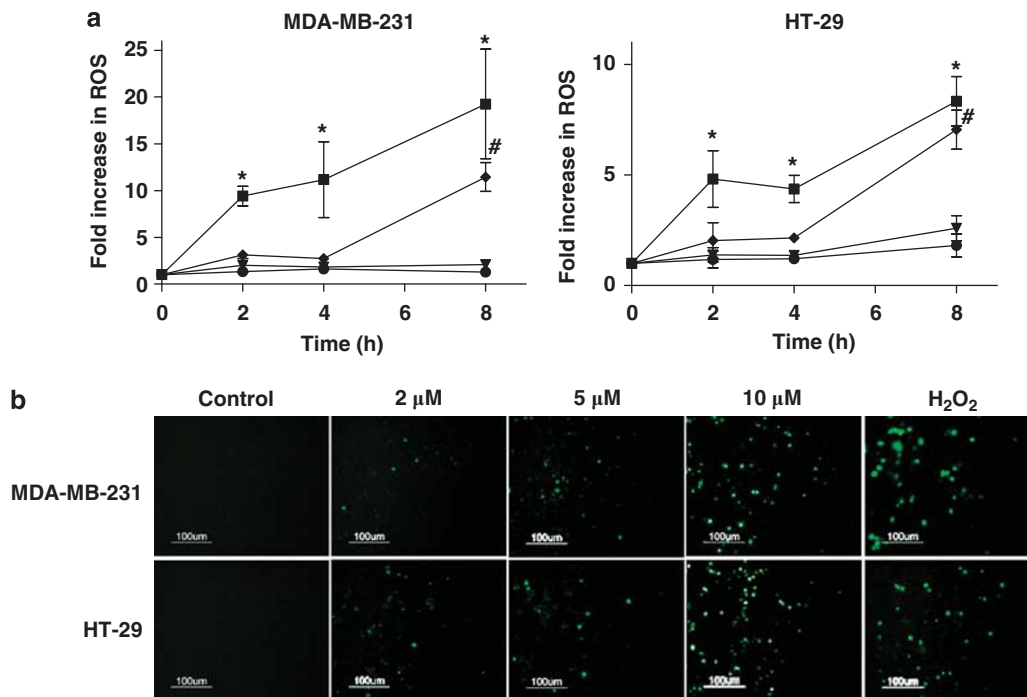

Figure 2 Detection of ROS by fluorescence intensity measurement using a microplate reader and fluorescence microscope. (**a**) Cells were treated with 2 μM (●), 5 μM (▼), 10 μM (◆) safingol and 200 μM H$_2$O$_2$ (■) for the indicated time before incubation with 5 μM H$_2$DCFDA. Fluorescence intensity was measured. In parallel, cell viability was monitored using WST-1. Fold increase in ROS production in treated cells was compared with untreated cells, and calculated by the equation as described in Materials and methods section. Each reported value represents the mean ± S.E.M. from three independent experiments (*,[#]P < 0.05, compared with untreated control). (**b**) Cells were treated with 2, 5 and 10 μM safingol and H$_2$O$_2$ for 8 h. After incubation with 5 μM H$_2$DCFDA, cells were washed and examined by fluorescence microscope. Representative images of cells from three independent experiments were shown. Bar = 100 μm

Figure 3 Induction of autophagy in MDA-MB-231 and HT-29 cells. (**a**) Ultrastructural features of safingol-treated cells. MDA-MB-231 cells were treated with 5 μM safingol while HT-29 cells were treated with 10 μM safingol for 24 h. Cells were harvested, fixed and observed under transmission electron microscopy. Representative images of cells from three independent experiments with different magnification and scale bars were shown. (**a**) Control; (**b–d**) safingol-treated cells. *N* indicates nucleus; *M* indicates mitochondria; arrow indicates double membrane structure. (**b**) Detection of AVO in safingol-treated cells. Cells were treated with safingol ± 1 mM 3-MA for 24 h before stained with 1 μg/ml acridine orange for 15 min. Cells were examined by fluorescence microscopy. Representative images of cells from three independent experiments were shown. Bar = 50 μm. (**c**) Concentration-dependent upregulation of LC3-II after safingol treatment for 48 h. (**d**) Time-dependent upregulation of LC3-II, Atg 7, Atg 5 and Atg 12 expression after 10 μM safingol treatment. Protein lysates were collected and assayed by western blotting. β-Actin was used as the loading control. All blots shown are representative of three independent experiments. Lower panels show the densitometric analysis where the band intensities of the proteins under investigation were normalized to that of β-actin in the respective cell lines. Results shown are means ± S.E.M. from three independent experiments. (*P < 0.05, compared with t = 0 h)

correlating the amount of oxidized cellular proteins with the induction of autophagy would provide further insights into the catabolic role of autophagy on safingol treatment.

To further substantiate the role ROS has in safingol-induced cancer cell death, we examined the viability of MDA-MB-231 and HT-29 cells in the presence and absence of the
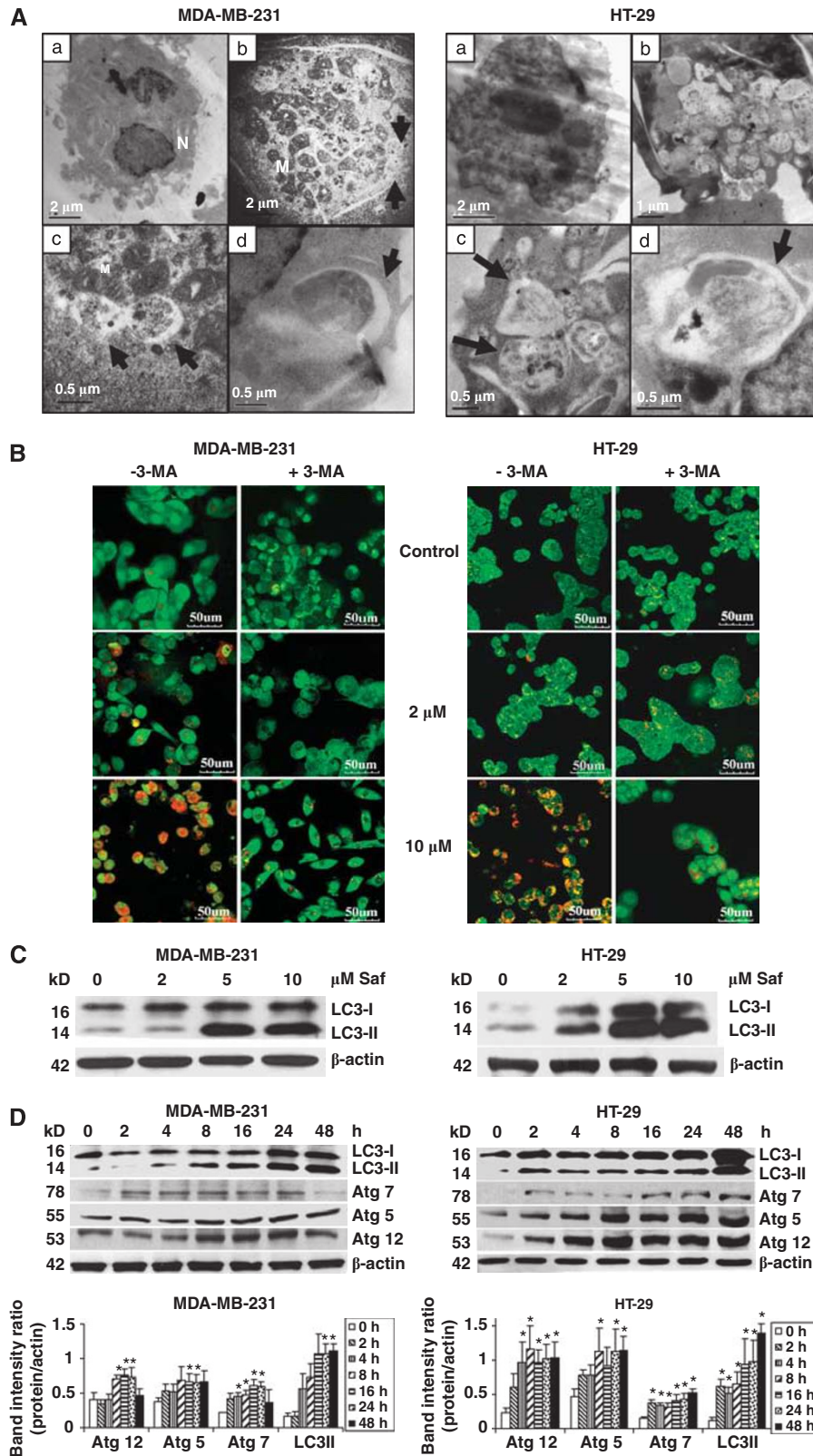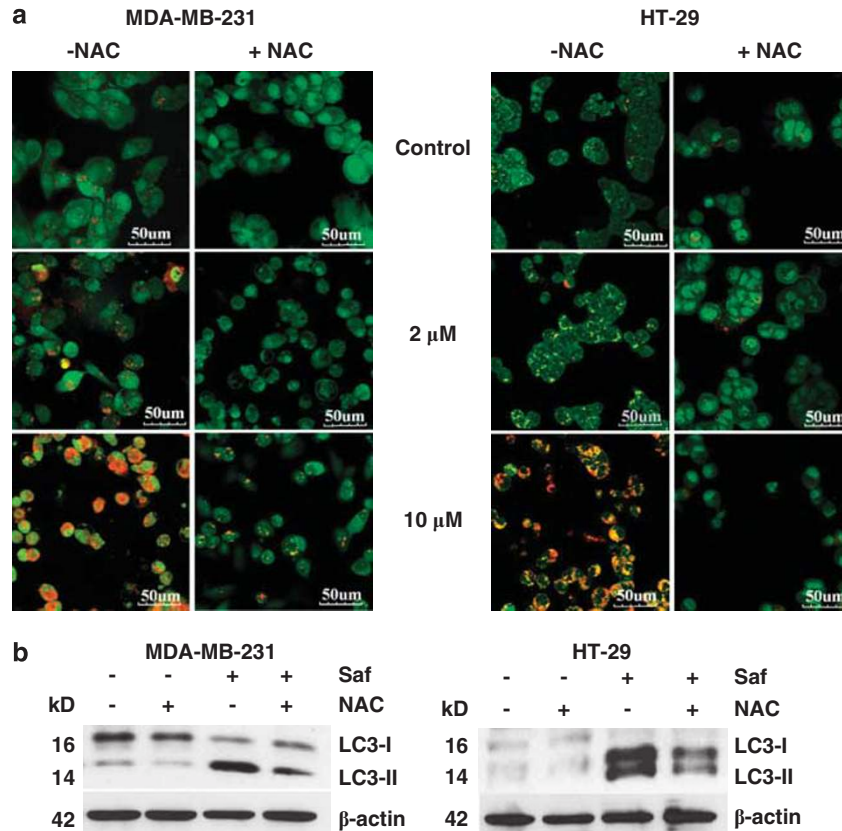
Figure 4 ROS trigger autophagy induction in MDA-MB-231 and HT-29 cells. (**a**) Detection of AVO in safingol-treated cells in the presence of NAC. Cells were treated with safingol ± 10 mM NAC for 24 h before stained with 1 μg/ml acridine orange for 15 min. Cells were examined by fluorescence microscopy. Representative images of cells from three independent experiments were shown. Bar = 50 μm. (**b**) Downregulation of LC3-II in cells in the presence of NAC. Cells were treated with safingol ± 10 mM NAC for 48 h. Protein lysates were assayed by western blotting and β-actin was used as the loading control. All blots shown are representative of three independent experiments

ROS scavenger, NAC. Indeed, on removal of ROS by NAC, the percentage of safingol-treated cells stained positive for 7AAD was significantly reduced from 86.9 to 14.6% for MDA-MB-231 and from 68.4 to 42.4% for HT-29 (Figure 5b). Taken together, our data indicate that ROS have an important role in mediating safingol-induced autophagy and necrotic cell death.

Bcl-xL and Bax regulates safingol-induced autophagy. On the basis of the recent findings that Bcl-2 homologues regulate autophagy by binding directly to beclin-1, which is an autophagy-inducing protein that contains a Bcl-2 homology 3 domain,[24,31] we examined the involvement of beclin-1, Bcl-xL and Bax in safingol-induced autophagy. Specifically, the ratios of beclin-1/Bcl-xL expression were determined instead of the changes in expression levels of the individual proteins, as the ratio of beclin-1/Bcl-xL expression is important to the regulation of autophagy – a mechanism that is analogous to the regulation of apoptosis by the Bcl-2 protein family, which is based on the ratio of pro-apoptotic/anti-apoptotic proteins. From Figure 6a, significant increases in the ratio of beclin-1/Bcl-xL were observed at 24 and 48 h for MDA-MB-231 cells and at 48 h for HT-29 cells. A concomitant increase in Bax expression was also observed.

Stemming from the results in Figure 6a, we hypothesized that the use of gossypol, which is an inhibitor of Bcl-xL could possibly suppress the Bcl-xL-mediated inhibitory effect on autophagy and thereby promoting the occurrence of autophagy. Results from Figure 6b are consistent with this notion, whereby an increase in AVO formation could be observed in the presence of gossypol when the cells were treated with safingol. In light of the results presented in Figures 2-5, autophagy is likely to be a catabolic process triggered by ROS overproduction on safingol treatment, we thus further hypothesized that inhibition of Bcl-xL by gossypol would have less suppressive effect on autophagy, which in turn would possibly result in more catabolism of ROS-damaged cellular components and promotion of cell survival. Consistent with this hypothesis, it was found that gossypol-treated cells became less sensitive to safingol treatment, as reflected by significant increases in IC_{50} values (Figure 6c). However, the regulatory mechanism of autophagy is complex that involves multiple signaling pathways, and it is possible that the use of gossypol could affect other molecular signals that contribute to the regulation of autophagy in addition to modulation of Bcl-xL.

Safingol reduced glucose uptake. Our results thus far suggest that ROS generation mediates safingol-induced
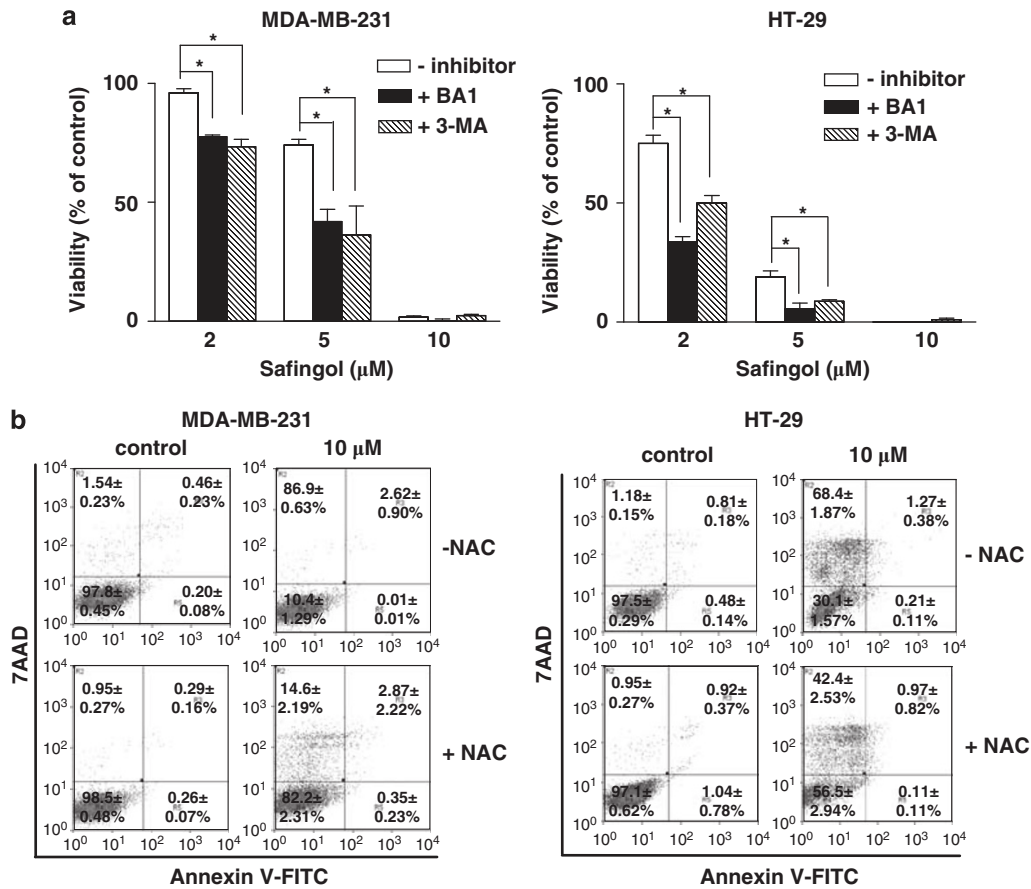
Figure 5 The role of autophagy and ROS in safingol-treated cells. (**a**) Effect of autophagy inhibitors on the viability of safingol-treated cells. Cells were treated with safingol for 24 h before the incubation with 1 mM 3-MA or 5 nM BA1 for additional 48 h. Cell viability was assessed using MTT assay. Results shown are means ± S.E.M. from three independent experiments (*$P < 0.05$, compared with untreated control). (**b**) Flow cytometric analysis of MDA-MB-231 and HT-29 cells after treated with 10 μM safingol ± 10 mM NAC for 48 h. Cells were harvested and stained with annexin V-FITC/7AAD before analyzed by flow cytometry. Representative dot plots are shown and each reported value represents the mean ± S.E.M. from three independent experiments

cancer cell death. It is therefore of interest to investigate how safingol induced ROS generation in these cells. Previously, sphingolipids have been shown to inhibit glucose uptake,[32,33] which could in turn induce oxidative stress.[34] These reports provided the basis for us to hypothesize that safingol, a synthetic sphingolipid, might be able to inhibit glucose uptake. Using a fluorescent derivative of glucose, 2-(N-(7-nitrobenz-2-oxa-1,3-diazol-4-yl)amino)-2-deoxyglucose (2-NBDG), the uptake was probed in MDA-MB-231 and HT-29 cells. Our results showed that 10 μM safingol significantly inhibited 2-NBDG uptake in both cell lines as early as 2 h (Figure 7a), preceding the generation of ROS (Figure 2).

Considering the finding that AMP-activated protein kinase (AMPK) and mammalian target of rapamycin (mTOR) are critical energy sensors that also have a role in autophagy regulation,[35] the effect of safingol on the phosphorylation of AMPK and mTOR was examined. As shown in Figure 7b, 10 μM safingol caused a rapid and significant increase in AMPK phosphorylation at 2 h in both cell lines, which is in line with the observation that safingol inhibited glucose uptake (Figure 7a). The expression of phosphorylated mTOR was initially increased in safingol-treated MDA-MB-231 and HT-29

cells, which was subsequently reduced at 24 and 48 h (Figure 7b). The initial increase in phosphorylated mTOR is intriguing and warrants further investigation, which could shed new light on the possible involvement of other signals that regulate the expression of phosphorylated mTOR during autophagy induction in addition to AMPK.

Discussion

To our knowledge, this is the first report showing that ROS have a key role in safingol-treated human cancer cell lines, MDA-MB-231 and HT-29. Interestingly, such ROS production could also trigger autophagy, which appeared to be a repair mechanism. We have also shown that glucose uptake is inhibited by safingol, which is an event preceding ROS generation. On the basis of these findings, we propose a model depicting the possible mechanism of action of safingol in MDA-MB-231 and HT-29 cells (Figure 8).

Regardless of how and where ROS are generated, a rise in ROS levels has two potential consequences: damage to cellular components and triggering various signaling pathways.[1] Here, we show that accumulation of ROS is essential for safingol-induced cell death as such death can be largely
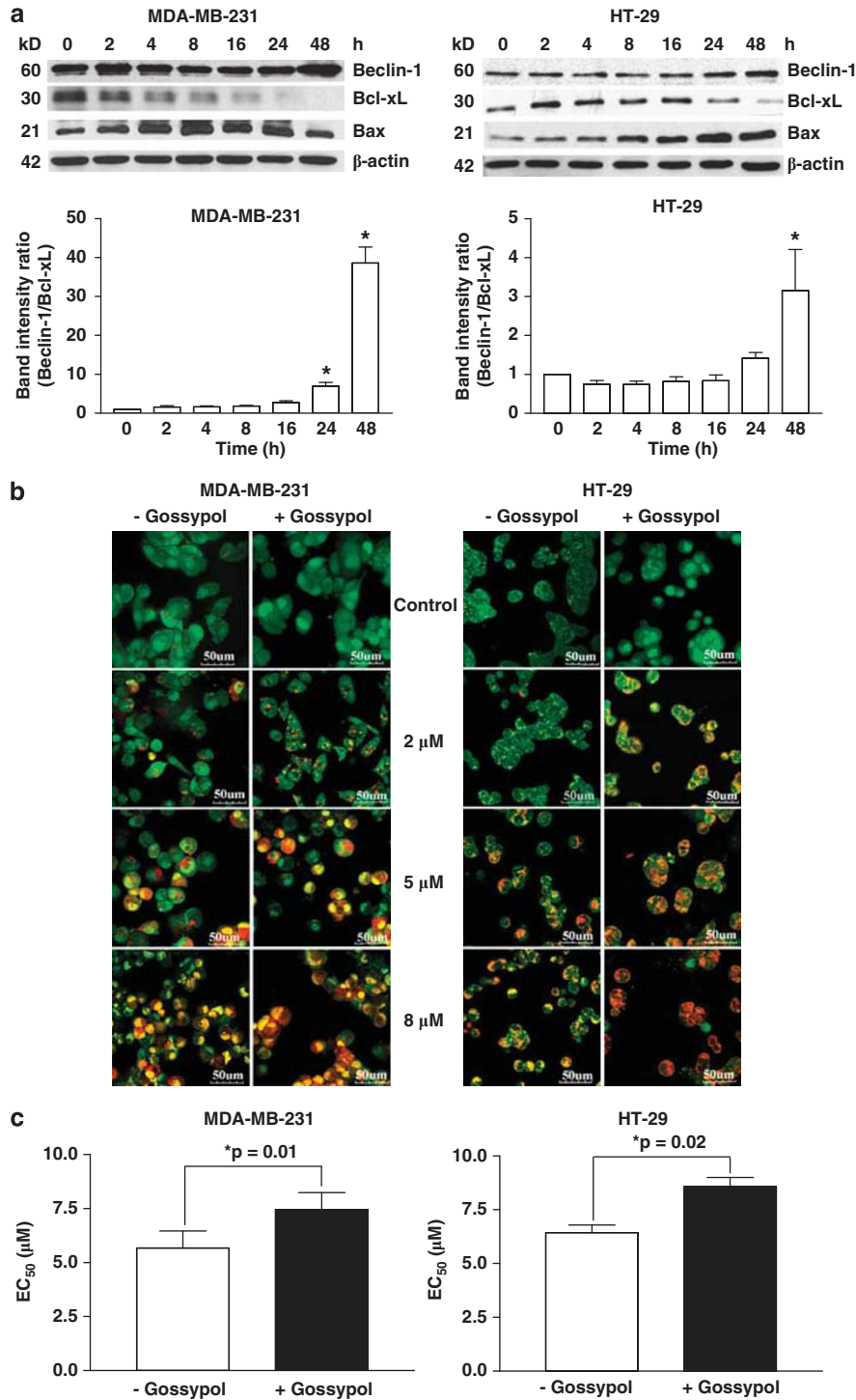
Figure 6 Regulation of autophagy by beclin-1, Bcl-xL and Bax in safingol-treated MDA-MB-231 and HT-29 cells. (a) The involvement of beclin-1, Bcl-xL and Bax in safingol-treated cells. Cells were treated with 10 μM safingol for the indicated time. Protein lysates were assayed by western blotting and β-actin was used as the loading control. All blots shown are representative of three independent experiments. Lower panels show the densitometric analysis where the band intensities of the proteins under investigation were normalized to that of β-actin. Results shown are mean ratios of beclin-1 to Bcl-xL $\pm$ S.E.M. from three independent experiments. (*$P < 0.05$, compared with $t = 0$ h). (b) Detection of AVO in safingol-treated cells in the presence of Bcl-xL inhibitor, gossypol. Cells were treated with safingol $\pm$ 5 μM gossypol for 24 h before stained with 1 μg/ml acridine orange for 15 min. Cells were examined by fluorescence microscopy. Representative images of cells from three independent experiments were shown. Bar = 50 μm. (c) Effect of gossypol on the viability of safingol-treated cells. Cells were treated with safingol $\pm$ 5 μM gossypol for 24 h. Cell viability was assessed using MTT assay. Results shown are means $\pm$ S.E.M. from three independent experiments
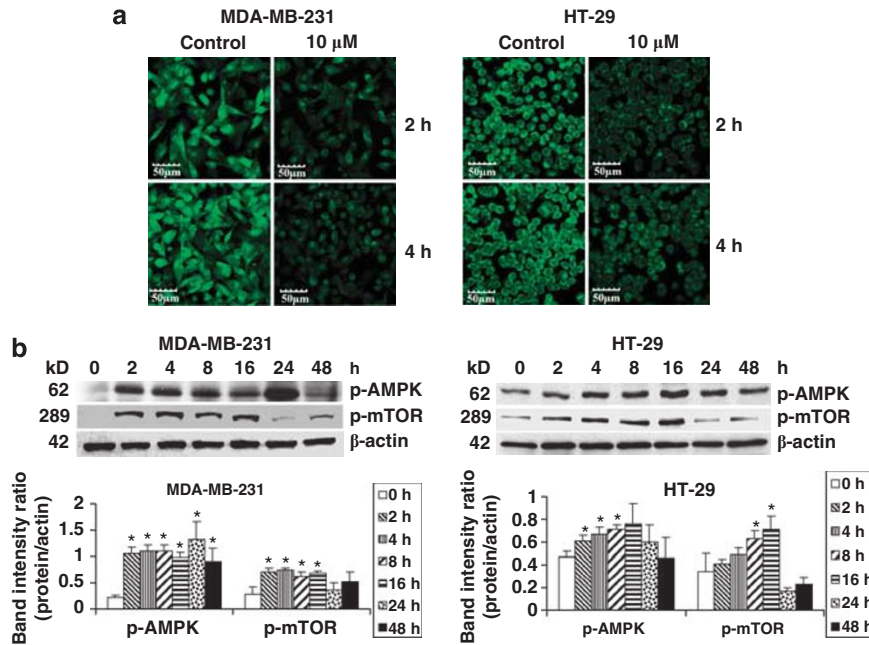
Figure 7 (a) Effect of safingol on glucose uptake in MDA-MB-231 and HT-29 cells. Cells were cultured in glucose-free media for 24 h before treated with 10 μM safingol for the indicated time. Cells were incubated with a fluorescent glucose derivative, 2-NBDG, for 30 min before examination by fluorescence microscopy under similar conditions. Representative images of cells from three independent experiments were shown. Bar = 50 μm. (b) Expression levels of p-AMPK and p-mTOR in safingol-treated MDA-MB-231 and HT-29 cells. Cells were treated with 10 μM safingol for the indicated time. Protein lysates were assayed by western blotting and β-actin was used as the loading control. All blots shown are representative of three independent experiments. Lower panels show the densitometric analysis where the band intensities of the proteins under investigation were normalized to that of β-actin in the respective cell lines. Results shown are means ± S.E.M. from three independent experiments (*$P < 0.05$, compared with $t = 0$ h)
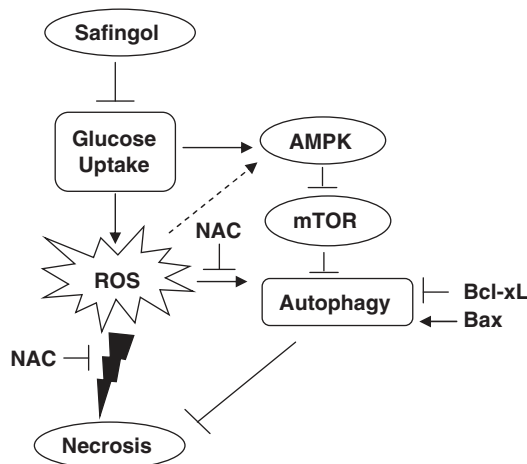

Figure 8 Proposed model depicting the mechanism of action of safingol in MDA-MB-231 and HT-29 cells

prevented by NAC. However, in *Aspergillus nidulans*, Cheng *et al.*[21] reported that the fungicidal activity of safingol does not require ROS, despite a rapid accumulation of ROS was observed. Such discrepancy is likely due to the difference in cancer cell response compared with that of fungi. In addition, we found that ROS generation is a relatively early event, suggesting that ROS could be the mediator leading to the loss of MMP, possibly by triggering the opening of the mitochondria permeability transition pore that subsequently leads to cell death. Our results also demonstrated that safingol-treated

cells undergo accidental necrotic cell death, as reflected by the caspase-independent cell death, rupture of plasma membrane integrity, loss of MMP and depletion of ATP, but not the involvement of RIP1 kinase. By targeting a non-apoptotic cell death pathway, safingol might provide an alternative strategy for developing combination therapies, in particular to eliminate cells, which are resistant to apoptotic cell death.

In line with two previous studies,[17,18] our results have demonstrated that safingol induced autophagy, possibly being regulated by Bcl-2 family proteins. The downregulation of Bcl-xL and upregulation of Bax observed in our study is consistent with the finding that arsenic trioxide induced autophagy in U118 human glioma cells in the absence of apoptosis, despite being regulated by Bcl-2 family proteins.[36] Parallel with this, studies have illustrated the binding of Bcl-xL and Bcl-2 to beclin-1, thus preventing autophagy.[24] On the other hand, Bax activation has been shown to induce autophagy, which is Atg 5-, Atg7- and Atg10-dependent.[25] Although safingol-induced autophagy has been clearly demonstrated, it is yet to unveil whether such autophagy directly contributes to death or is a failed effort to preserve cell viability. Our results suggest the latter, where autophagy functions possibly as a mechanism to remove damaged organelles and proteins in response to safingol-induced oxidative stress. In addition to supporting the current knowledge that ROS regulates autophagy,[5] our data are also in line with findings that demonstrated the protective role of autophagy induced by sphingolipids in cell death, especially during nutrient starvation.[37]

Consistent with our study, short-chain fatty acids were shown to induce ROS production, which led to AMPK activation and consequential mTOR inhibition.[38] Our results offer an explanation that glucose uptake inhibition by safingol could be one of the factors leading to an increase in AMPK phosphorylation in parallel with ROS generation. Under metabolic stresses, such as glucose deprivation, AMPK is activated to increase catabolism, either by direct phosphorylation of metabolic enzymes or regulation of transcription.[39] Similarly, glucose deprivation was shown to initiate oxidative stress and increase mitochondria production of ROS, as demonstrated in lung cancer cells A549, brain cells, retina cells and adrenal cells.[34] Although several *in vivo* studies supported the upstream role of ROS in activating AMPK,[40] this remains to be determined in safingol-treated cells. AMPK is not only known as an energy sensor, but also reported to have a role in inducing autophagy through the suppression of mTOR.[35] However, in our study, the initial increase in phosphorylated mTOR is intriguing that warrants further investigation, which could yield new insights into the signals in the regulation of phosphorylated mTOR expression during autophagy induction. Of note, it has been shown that the PI3k/Akt/mTOR pathway was involved in regulating safingol-induced autophagy.[17] Thus, the PI3k/Akt pathway could be involved in regulating p-mTOR expression in addition to AMPK. The direct effect of AMPK and mTOR on safingol-induced autophagy could be further studied with pharmacological activators and inhibitors of AMPK and mTOR so as to tease out the contribution of AMPK-mTOR signaling in safingol-induced autophagy and necrosis.

In summary, our studies provide experimental evidence that ROS have a key role in mediating the cytotoxicity of safingol in cancer cells. It is worthwhile to note that depending on the magnitude and the duration of exposure, ROS can elicit different responses. Safingol at 2 and 5 μM resulted in low levels of ROS production, and autophagy was possibly induced to remove oxidatively damaged organelles. However, at 10 μM safingol treatment, high levels of ROS were produced and possibly exceeded the cells' repair capacity and thus leading to cell death by necrosis. Together, these data suggest that safingol may be an attractive agent to combine with apoptotic- and ROS-generating anticancer drugs at appropriate concentrations to treat potential drug-resistant cancers. It is anticipated that such combinations of drugs may show synergistic effect by executing different modes of cell death.

Materials and Methods

Reagents. Safingol was purchased from Sigma-Aldrich (St. Louis, MO, USA) and dissolved in ethanol. Stock solutions of 2 mg/ml were stored at −20 °C and freshly diluted with medium to the appropriate concentrations before use in experiments. All other chemicals used in the study were purchased from Sigma-Aldrich unless otherwise stated.

Cell cultures. Two human cancer cell lines, MDA-MB-231 and HT-29, were purchased from American Type Culture Collection (Manassas, VA, USA). Stock cultures of both cancer cell lines were maintained as monolayer in 75-cm^2 tissue culture flasks (Iwaki, Japan). MDA-MB-231 cells were cultured in Roswell Park Memorial Institute 1640 (RPMI-1640) medium while HT-29 in Iscove's modified Dulbecco's medium. All media were supplemented with 10% v/v fetal bovine serum (HyClone Laboratories, Logan, UT, USA), 0.3 g/l L-glutamine, 100 U/ml penicillin and 100 μg/ml streptomycin. The cell lines were maintained in a humidified, 5% CO$_2$

incubator at 37 °C and sub-cultured twice weekly using 0.25% v/v trypsin/EDTA (GIBCO, Grand Island, NY, USA). All experiments were performed using cells in exponential growth phase from passage 5 to 20 post-thawing from frozen stock.

Cell viability assay. Viability of the cancer cells following drug treatment was determined using the colorimetric 3-(4,5-dimethylthiazol-2-yl)-2,5-diphenyl tetrazolium bromide (MTT) assay. In brief, cells were plated at 5000 per well in 96-well plates and allowed to adhere overnight before exposure to safingol ± inhibitors/agents. The plates were then incubated for specified period at 37 °C. At the end of the incubation, 50 μl MTT (1 mg/ml in media) was added to cells and incubated for 4 h. Subsequently, the MTT-containing medium was removed, and the purple formazan precipitate was solubilized in DMSO with shaking. Absorbance reading ($\lambda = 570$ nm) was measured using a microtiter plate reader (Tecan, Infinite 200 PRO, Tecan Group Ltd, Mannedorf, Switzerland). All assays were done at least three times unless otherwise stated.

Cancer cell viability was calculated based on the absorbance readings using the following equation: viability = $((\text{Abs}_{test} - \text{Abs}_{blank})/(\text{Abs}_{vehicle\ control} - \text{Abs}_{blank}))$ $\times 100\%$, where Abs_{test}, Abs_{blank}, $\text{Abs}_{vehicle\ control}$ represent the absorbance readings from the drug-treated wells, the medium only wells and the vehicle control wells, respectively.

Flow cytometry with annexin V-FITC/7AAD staining. In brief, 1.5×10^6 cells were seeded and treated with various concentrations of safingol ± 10 mM NAC in MDA-MB-231 and 2.5 mM NAC in HT-29 cells for 48 h. 2% paraformaldehyde was used as a positive control for inducing cell death with necrotic features. After drug exposure, cells were harvested, washed with ice-cold phosphate-buffered saline (PBS), and stained with annexin V-FITC/7AAD kit (Beckman Coulter, Villepinte, France) for 15 min in dark. In all, 450 μl of binding buffer were added to terminate the reaction. The samples were kept on ice before subjected to flow cytometric analysis. Stained samples were analyzed on the Dako flow cytometer (Dako Cytomation Cyan LX, Dako Corp., Carpinteria, CA, USA) and 10 000 events were collected. Data were plotted with Summit V4.3 Build 2445 software (Dako Colorado Inc., Fort Collins, CO, USA).

MMP measurement. In all, 1.5×10^6 cells were seeded in T-75 flasks and treated for 8, 24 and 48 h with 10 μM safingol. Then, 1×10^5 cells were harvested and incubated with 100 μl 5,5′,6,6′ tetrachloro-1,1′,3,3′-tetraethylbenzimidazolyl-carbocyanine iodide (JC-1) at a final concentration of 1 μg/ml for 30 min at 37 °C. In healthy cells, JC-1 stains the mitochondria red whereas in cells with collapsed MMP, JC-1 remains in the cytoplasm and emits green fluorescence. After staining, cells were washed twice with ice-cold PBS and subjected to flow cytometry analyses using Dako flow cytometer model CyAn ADP, and 10 000 events were collected. Data were plotted with Summit V4.3 Build 2445 software.

ATP measurement. In total, 10^5 cells per well were plated in black 96-well plates and allowed to adhere for 24 h. Following 48-h treatment with 2, 5 and 10 μM safingol, ATP levels were measured using the ATP bioluminescence assay kit HSII (Roche Diagnostics, Indianapolis, IN, USA) according to the manufacturer's instruction.

ROS measurement. ROS measurement was performed using H$_2$DCFDA according to the manufacturer's instructions. In brief, each 96-well plates was seeded with 2×10^4 cells per well and allowed to adhere overnight. In all, 2, 5 and 10 μM safingol was added for the indicated period. H$_2$O$_2$ was used as a positive control. Following the drug treatment, media was removed and cells were loaded with 5 μM H$_2$DCFDA diluted in clear media for 30 min at 37 °C. Cells were washed three times with clear media and fluorescence intensity (excitation = 485 nm; emission = 530 nm) was measured using a microtiter plate reader (Tecan, Infinite M2000). Morphology of cells was photographed using Nikon ECLIPSE TE2000-U (Nikon Instruments Inc., Melville, NY, USA) microscope. Finally, 100 μl of premixed WST-1 cell proliferation reagent (Clontech Laboratories Inc., Mountain View, CA, USA) was added to determine the cell viability. Abs was measured at $\lambda = 440$ nm in a microplate reader (Tecan, Infinite 2000). Folds increased in ROS production was calculated using the following equation: $(F_{test} - F_{blank})/(F_{control} - F_{blank})$, where F_{test}, F_{blank}, $F_{control}$ represent the fluorescence readings from the drug-treated wells, the unstained cells and the stained control wells, respectively.

Electron microscopy. Briefly, cells were treated with safingol for 24 and 48 h, harvested by trypsinization, washed twice with PBS and pre-fixed with ice-cold 2.5% v/v glutaraldehyde and 2% v/v paraformaldehyde in buffer for 3 h. After washing three

times with PBS, cells were post-fixed in 1% osmium tetroxide in dark for 2 h. A series of graded dehydration was carried out, followed by embedding of cells in Spurr's resin. In all, 90 nm thin sections were cut, stained with Hiraoka staining kit (Polyscience Inc., Warrington, PA, USA) and viewed with PHILIPS CM10 (Phillips Electronics, Mahway, NJ, USA) transmission electron microscope.

Acridine orange staining. Staining of cells with acridine orange was performed according to published procedures.[28] In brief, acridine orange at a final concentration of 1 mg/ml was added to treated-cells for a period of 20 min at 37 °C. Then, cells were washed twice with PBS. Images of cells were obtained using Olympus FluoView FV300 (Olympus Inc., Melville, NY, USA) confocal microscope.

Western blotting. Cells were exposed safingol for the specified concentrations and duration. In some experiments, cells were treated in the presence of NAC. After drug treatment, cells were washed with ice-cold PBS and lysed in ice-cold cell lysis buffer (20 mM Tris pH 7.5, 150 mM NaCl, 10 mM EDTA, 1% w/v NP-40, 20 mM sodium fluoride, 5 mM sodium pyrophosphate, 1 mM sodium vanadate, 10% v/v glycerol, 1 × protease inhibitor cocktail) just before use. Protein concentration was determined using the Bio-Rad Protein Assay Kit (Bio-Rad Laboratories, Hercules, CA, USA). Proteins were separated by electrophoresis carried out on 1.5-mm thick, 6 to 12% sodium dodecyl sulfate-polyacrylamide gels using Bio-Rad's Powerpac HC Apparatus (Bio-Rad Laboratories, Singapore) and electroblotted onto nitrocellulose membranes in ice-cold transfer buffer (39 mM glycine, 48 mM Tris base, 20% v/v methanol). The membranes were subsequently blocked with 5% w/v bovine serum albumin (BSA; Sigma-Aldrich) in Tris-buffered saline with 0.1% v/v Tween 20 (TBS/T) for 2 h. The membranes were then probed with primary antibodies overnight at 4 °C. Primary rabbit polyclonal LC3-II, beclin-1, Bcl-xL, Bax, p-AMPKα (Thr 172) and p-mTOR (Ser2448) antibodies were purchased from Cell Signaling Technology, Inc. (Danvers, MA, USA) and diluted with TBS/T in 1 : 1000 ratio containing 5% w/v BSA. Membranes were probed with horseradish peroxidase-conjugated goat anti-rabbit antibody (Pierce Biotechnology, Rockford, IL, USA) for another hour, followed by detection with chemi-luminescence Supersignal West Dura Extended Duration Substrate (Pierce Biotechnology, Rockford, IL, USA). β-Actin was included as the loading control. The intensities of the individual bands were determined by densitometry (Image J 1.43u, National Institutes of Health, Bethesda, MD, USA).

Glucose uptake assay. Cells were plated at 2×10^4 per well and allowed to adhere overnight. On the following day, cell culture medium was removed and replaced by glucose-free medium for 24 h. Then, safingol at 10 μM was added to cells for the indicated time. At the end of safingol treatment, 0.3 mM of 2-NBDG (Invitrogen, Eugene, OR, USA) diluted in Hanks-buffered salt solution (HBSS) was added into each well for 30 min at 37 °C. The 2-NBDG uptake reaction was stopped by removing the medium and washing the cells twice with HBSS. Images of cells were obtained using Olympus FluoView FV300 confocal microscope.

Statistical analysis. All data values were reported as mean ± S.E.M. Statistical differences were determined using the Student's t-test or one-way analysis of variance with Dunnett's test used for post hoc multiple comparisons. P-values of < 0.05 were considered to be statistically significant.

Conflict of interest

The authors declare no conflict of interest.

1. Finkel T, Holbrook NJ. Oxidants, oxidative stress and the biology of ageing. Nature 2000; **408**: 239–247.
2. Azad MB, Chen Y, Gibson SB. Regulation of autophagy by reactive oxygen species (ROS): implications for cancer progression and treatment. Antioxid Redox Signal 2009; **11**: 777–790.
3. Kroemer G, Galluzzi L, Vandenabeele P, Abrams J, Alnemri ES, Baehrecke EH et al. Classification of cell death: recommendations of the Nomenclature Committee on Cell Death 2009. Cell Death Differ 2009; **16**: 3–11.
4. Festjens N, Vanden Berghe T, Vandenabeele P. Necrosis, a well-orchestrated form of cell demise: signalling cascades, important mediators and concomitant immune response. Biochim Biophys Acta 2006; **1757**: 1371–1387.
5. Scherz-Shouval R, Elazar Z. ROS, mitochondria and the regulation of autophagy. Trends Cell Biol 2007; **17**: 422–427.
6. Buehrer B, Bell R. Sphingosine kinase: properties and cellular functions. Adv Lipid Res 1993; **26**: 59–67.
7. Schwartz G, Farsi K, Maslak P, Kelsen D, Spriggs D. Potentiation of apoptosis by flavopiridol in mitomycin-C-treated gastric and breast cancer cells. Clin Cancer Res 1997; **3**: 1467–1472.
8. Kedderis L, Bozigian H, Kleeman J, Hall R, Palmer T, Harrison SJ et al. Toxicity of the protein kinase C inhibitor safingol administered alone and in combination with chemotherapeutic agents. Fundam Appl Toxicol 1995; **25**: 201–217.
9. Carvajal RD. A phase I clinical trial of safingol followed by cisplatin: promising activity in refractory adrenocortical cancer with novel pharmacology. Proc Am Soc Clin Oncol 2006; **24**: 13044.
10. Hoffmann T, Leenen K, Hafner D, Balz V, Gerharz C, Grund A et al. Antitumor activity of protein kinase C inhibitors and cisplatin in human head and neck squamous cell carcinoma lines. Anticancer Drugs 2002; **13**: 93–100.
11. Jarvis W, Fornari FJ, Tombes R, Erukulla R, Bittman R, Schwartz G et al. Evidence for involvement of mitogen-activated protein kinase, rather than stress-activated protein kinase, in potentiation of 1-beta-D-arabinofuranosylcytosine-induced apoptosis by interruption of protein kinase C signaling. Mol Pharmacol 1998; **54**: 844–856.
12. Maurer B, Melton L, Billups C, Cabot M, Reynolds C. Synergistic cytotoxicity in solid tumor cell lines between N-(4-hydroxyphenyl)retinamide and modulators of ceramide metabolism. J Natl Cancer Inst 2000; **92**: 1897–1909.
13. Sachs C, Safa A, Harrison S, Fine R. Partial inhibition of multidrug resistance by safingol is independent of modulation of P-glycoprotein substrate activities and correlated with inhibition of protein kinase C. J Biol Chem 1995; **270**: 26639–26648.
14. Schwartz G, Haimovitz-Friedman A, Dhupar S, Ehleiter D, Maslak P, Lai L et al. Potentiation of apoptosis by treatment with the protein kinase C-specific inhibitor safingol in mitomycin C-treated gastric cancer cells. J Natl Cancer Inst 1995; **87**: 1394–1399.
15. Ling LU, Lin H, Tan KB, Chiu GN. The role of protein kinase C in the synergistic interaction of safingol and irinotecan in colon cancer cells. Int J Oncol 2009; **35**: 1463–1471.
16. Hannun Y, Loomis C, Merrill AJ, Bell R. Sphingosine inhibition of protein kinase C activity and of phorbol dibutyrate binding in vitro and in human platelets. J Biol Chem 1986; **261**: 12604–12609.
17. Coward J, Ambrosini G, Musi E, Truman JP, Haimovitz-Friedman A, Allegood JC et al. Safingol (L-threo-sphinganine) induces autophagy in solid tumor cells through inhibition of PKC and the PI3-kinase pathway. Autophagy 2009; **5**: 184–193.
18. Morales P, Dillehay D, Moody S, Pallas D, Pruett S, Allgood J et al. Safingol toxicology after oral administration to TRAMP mice: demonstration of safingol uptake and metabolism by N-acylation and N-methylation. Drug Chem Toxicol 2007; **30**: 197–216.
19. Noda T, Iwai S, Hamada M, Fujita Y, Yura Y. Induction of apoptosis of detached oral squamous cell carcinoma cells by safingol. Possible role of Bim, focal adhesion kinase and endonuclease G. Apoptosis 2009; **14**: 287–297.
20. Hamada M, Sumi T, Iwai S, Nakazawa M, Yura Y. Induction of endonuclease G-mediated apoptosis in human oral squamous cell carcinoma cells by protein kinase C inhibitor safingol. Apoptosis 2006; **11**: 47–56.
21. Cheng J, Park TS, Chio LC, Fischl AS, Ye XS. Induction of apoptosis by sphingoid long-chain bases in Aspergillus nidulans. Mol Cell Biol 2003; **23**: 163–177.
22. Shi L, Bielawski J, Mu J, Dong H, Teng C, Zhang J et al. Involvement of sphingoid bases in mediating reactive oxygen intermediate production and programmed cell death in Arabidopsis. Cell Res 2007; **17**: 1030–1040.
23. Villena J, Henriquez M, Torres V, Moraga F, Diaz-Elizondo J, Arredondo C et al. Ceramide-induced formation of ROS and ATP depletion trigger necrosis in lymphoid cells. Free Radic Biol Med 2008; **44**: 1146–1160.
24. Pattingre S, Tassa A, Qu X, Garuti R, Liang XH, Mizushima N et al. Bcl-2 antiapoptotic proteins inhibit Beclin 1-dependent autophagy. Cell 2005; **122**: 927–939.
25. Yee KS, Wilkinson S, James J, Ryan KM, Vousden KH. PUMA- and Bax-induced autophagy contributes to apoptosis. Cell Death Differ 2009; **16**: 1135–1145.
26. Amin H, Ergin M, Denning M, Quevedo M, Alkan S. Characterization of apoptosis induced by protein kinase C inhibitors and its modulation by the caspase pathway in acute promyelocytic leukaemia. Br J Haematol 2000; **110**: 552–562.
27. Degterev A, Hitomi J, Germscheid M, Ch'en IL, Korkina O, Teng X et al. Identification of RIP1 kinase as a specific cellular target of necrostatins. Nat Chem Biol 2008; **4**: 313–321.
28. Kanzawa T, Kondo Y, Ito H, Kondo S, Germano I. Induction of autophagic cell death in malignant glioma cells by arsenic trioxide. Cancer Res 2003; **63**: 2103–2108.
29. Seglen PO, Gordon PB. 3-Methyladenine: specific inhibitor of autophagic/lysosomal protein degradation in isolated rat hepatocytes. Proc Natl Acad Sci USA 1982; **79**: 1889–1892.
30. Yamamoto A, Tagawa Y, Yoshimori T, Moriyama Y, Masaki R, Tashiro Y. Bafilomycin A1 prevents maturation of autophagic vacuoles by inhibiting fusion between autophagosomes and lysosomes in rat hepatoma cell line, H-4-II-E cells. Cell Struct Funct 1998; **23**: 33–42.
31. Liang XH, Kleeman LK, Jiang HH, Gordon G, Goldman JE, Berry G et al. Protection against fatal Sindbis virus encephalitis by beclin, a novel Bcl-2-interacting protein. J Virol 1998; **72**: 8586–8596.

32. Murray D, Hill M, Nelson D. Inhibitory action of sphingosine, sphinganine and dexamethasone on glucose uptake: studies with hydrogen peroxide and phorbol ester. *Life Sci* 1990; **46**: 1843–1849.

33. Nelson D, Murray D. Sphingolipids inhibit insulin and phorbol ester stimulated uptake of 2-deoxyglucose. *Biochem Biophys Res Commun* 1986; **138**: 463–467.

34. Isaev NK, Stelmashook EV, Dirnagl U, Plotnikov EY, Kuvshinova EA, Zorov DB. Mitochondrial free radical production induced by glucose deprivation in cerebellar granule neurons. *Biochemistry (Mosc)* 2008; **73**: 149–155.

35. Meijer AJ, Codogno P. AMP-activated protein kinase and autophagy. *Autophagy* 2007; **3**: 238–240.

36. Cheng TJ, Wang YJ, Kao WW, Chen RJ, Ho YS. Protection against arsenic trioxide-induced autophagic cell death in U118 human glioma cells by use of lipoic acid. *Food Chem Toxicol* 2007; **45**: 1027–1038.

37. Lavieu G, Scarlatti F, Sala G, Carpentier S, Levade T, Ghidoni R *et al.* Regulation of autophagy by sphingosine kinase 1 and its role in cell survival during nutrient starvation. *J Biol Chem* 2006; **281**: 8518–8527.

38. Tang Y, Chen Y, Jiang H, Nie D. The role of short-chain fatty acids in orchestrating two types of programmed cell death in colon cancer. *Autophagy* 2011; **7**: 235–237.

39. Hardie DG. AMP-activated/SNF1 protein kinases: conserved guardians of cellular energy. *Nat Rev Mol Cell Biol* 2007; **8**: 774–785.

40. Zou MH, Kirkpatrick SS, Davis BJ, Nelson JS, Wiles WGT, Schlattner U *et al.* Activation of the AMP-activated protein kinase by the anti-diabetic drug metformin *in vivo*. Role of mitochondrial reactive nitrogen species. *J Biol Chem* 2004; **279**: 43940–43951.